

TABLE I. Upper limit for widths of possible resonances of total spin J for a neutron energy of 1250 kev. The neutron energy spread Δ is taken as 5 kev. Resonances with widths greater than the values given would have been observed in the present experiment. For a neutron energy of 610 kev, Γ would be about half the tabulated values.

J	σ_R (barns)	Δ/Γ_{\max}	Γ_{\max} (ev)
1/2	2.5	16.5	303
3/2	5.0	35.5	141
5/2	7.5	55.0	91
7/2	10.0	83.5	60

function for incident neutron flux, one can place upper limits for the widths of the resonances if they exist. Table I gives, for various assumed J values, the maximum value for the width of a resonance not observable at a neutron energy of 1250 kev, i.e., one that would have resulted in a 5% dip in the transmission curve. The energy spread Δ has been taken as 5 kev. Since no resonance was observed near this energy, it is concluded that the postulated state in C^{13} must be narrower than the values given in Table I. At 610 kev the widths would be restricted to approximately one-half of the values shown in Table I.

Since some 660 points were taken in this experiment, and further since the results gave a smooth curve, a least-squares fit of the cross section by a function with only a few parameters gives a very accurate determination of the cross section in this region. The use of such

a procedure⁵ leads to the following power-series expansion for the cross section:

$$\sigma_T = 4.710 - (3.415)E + (1.649)E^2 - (0.2606)E^4,$$

where E is in Mev, σ_T is in barns, and the value of the cross section at zero energy was taken to be 4.710 barns.⁶ The rms error in this region is 0.075 barn or an average of 2.7%. While no data (other than the cross section at zero energy) below 500 kev were included in the fitting, the calculated curve lies within 3% of other measurements^{2,6,7} from 1 to 500 kev.

For energies greater than 1400 kev the expansion quickly diverges from the measured cross-section values because of the large fourth-power term.

ACKNOWLEDGMENTS

The authors wish to thank Ronald Amrein and Walter Ray for their help in many phases of this experiment, and Morris Firebaugh for helping with the experiment and for performing most of the necessary routine calculations.

⁵ A least-squares-fitting program for use on the IBM-704 computer was supplied to us by J. E. Monahan of this laboratory.

⁶ Comparison was made with the smooth curve through the experimental points given in *Neutron Cross Sections*, compiled by D. J. Hughes and R. Schwartz, Brookhaven National Laboratory Report BNL-325 (Superintendent of Documents, U. S. Government Printing Office, Washington, D. C., 1958), second edition.

⁷ C. Kimball, J. E. Monahan, and F. P. Mooring, Argonne National Laboratory Report ANL-5894, 1958 (unpublished), p. 28.

Dynamic Orientation of Nuclei by Forbidden Transitions in Paramagnetic Resonance*

C. D. JEFFRIES

Physics Department, University of California, Berkeley, California

(Received July 30, 1959)

Principally from the viewpoint of orienting radionuclei, this paper considers magnetically dilute paramagnetic ions in crystals for various cases in which there is a non-negligible radio-frequency transition probability for inducing a simultaneous flipping of an electron spin and a nuclear spin. These transitions, forbidden in zero order in high magnetic fields, may be provided by hyperfine interactions, and allow for direct dynamic nuclear orientation by applied rf fields. The transition probabilities are calculated for a general anisotropic spin Hamiltonian; thermal relaxation transitions are qualitatively discussed. The resulting steady-state dynamic nuclear polarization and alignment are calculated for the equalization of populations of pairs of levels by sufficient applied rf fields. The influence of various relaxation transitions is considered and it is noted that the nuclear orientation available through the forbidden transitions is considerably less sensitive to competing relaxation transitions than that obtained by saturation of the allowed transitions.

The general predictions are found to be in qualitative agreement with the results at Berkeley of Abraham and Kedzie using radionuclei.

The possibilities for dynamic alignment of radionuclei of diamagnetic atoms by forbidden transitions due to weak nuclear-electron dipolar coupling are also briefly discussed.

I. INTRODUCTION

OVERHAUSER¹ pointed out, and it was experimentally verified,² that the saturation of the

paramagnetic resonance transitions of the conduction electrons in a metal could, through suitable hfs relaxation processes, lead to an appreciable nuclear polarization. This idea has been extended³ to paramagnetic

* Supported in part by the U. S. Atomic Energy Commission and the Office of Naval Research.

¹ A. Overhauser, Phys. Rev. **89**, 689 (1953); **92**, 411 (1953).

² T. R. Carver and C. P. Slichter, Phys. Rev. **92**, 212 (1953).

³ F. Bloch, Phys. Rev. **93**, 944 (1954); A. Overhauser, Phys. Rev. **94**, 768 (1954); J. Korringa, Phys. Rev. **94**, 1388 (1954); C. Kittel, Phys. Rev. **95**, 589 (1954); P. Brovetto and G. Cini,

substances in general and many related proposals and experiments have been described. Abragam,⁴ in particular, has treated some cases of electron-nuclear coupled systems of general physical interest. The present paper is essentially an extension of Abragam's treatment with these specific differences: we here consider in detail the proposal⁵ of utilizing radio-frequency (rf) induced "forbidden transitions" in which electron and nuclear spins are simultaneously flipped; we consider a general anisotropic spin Hamiltonian; and our principal view is orientation of radionuclei for γ -ray anisotropy studies. In particular, this paper presents the theory for the experiments on Co⁶⁰ by Abraham et al.,⁶ and on Mn^{52,54} by Kedzie et al.⁷ which will be described in full detail in following papers.^{8,9}

All of the experiments referred to above may be described as dynamic nuclear orientation experiments. By this we mean that the normal Boltzmann populations of a system of spins in a lattice in a dc magnetic field is so changed by the application of resonant rf (including microwave frequencies) fields as to establish an appreciably greater degree of nuclear orientation than exists for the spins in thermal equilibrium with their lattice at the same temperature. The enhancement may be several orders of magnitude if the nuclear spins are coupled to electron spins.

The nuclear orientation for a spin I may be described by a series of $2I$ orientation parameters p_1, p_2, p_3, \dots , the first two of which are conveniently defined¹⁰ as the polarization:

$$p_1 = (1/I) \sum_i \langle \Psi_i | I_z | \Psi_i \rangle N_i / \sum_i N_i; \quad (1)$$

Nuovo cimento **11**, 618 (1954); P. Brovetto and S. Ferroni, Nuovo cimento **12**, 90 (1954); A. Abragam, Phys. Rev. **98**, 1729 (1955); A. Abragam, Compt. rend. **242**, 1720 (1956); F. Bloch, Phys. Rev. **102**, 104 (1956); G. Feher, Phys. Rev. **103**, 500 (1956); G. Feher and E. A. Gere, Phys. Rev. **103**, 834 (1956); C. D. Jeffries, Phys. Rev. **106**, 164 (1957); D. Pines, J. Bardeen, and C. P. Slichter, Phys. Rev. **106**, 489 (1957); F. M. Pipkin and J. W. Culvahouse, Phys. Rev. **106**, 1102 (1957); I. Solomon, J. Phys. Radium **19**, 837 (1958); J. Combrisson, J. phys. Radium **19**, 840 (1958); R. S. Codrington and N. Bloembergen, J. Chem. Phys. **29**, 600 (1958); A. Abragam and W. G. Proctor, Compt. rend. **246**, 2253 (1958); G. R. Khutsishvili, Nuovo cimento **11**, 186 (1959).

⁴ A. Abragam, Phys. Rev. **98**, 1729 (1955).

⁵ C. D. Jeffries, Phys. Rev. **106**, 164 (1957); C. D. Jeffries, *Proceedings of the Fifth International Conference on Low-Temperature Physics and Chemistry, Madison, Wisconsin, August, 1957*, edited by J. R. Dillinger (University of Wisconsin Press, Madison, 1958).

⁶ M. Abraham, R. W. Kedzie, and C. D. Jeffries, Phys. Rev. **106**, 165 (1957).

⁷ R. W. Kedzie, M. Abraham, C. D. Jeffries, and O. Leifson, Bull. Am. Phys. Soc. **2**, 382 (1957); R. W. Kedzie and C. D. Jeffries, Bull. Am. Phys. Soc. **3**, 415 (1958).

⁸ M. Abraham, C. D. Jeffries, and R. W. Kedzie, Phys. Rev. **117**, 1070 (1960).

⁹ R. W. Kedzie (to be published).

¹⁰ R. J. Blin-Stoyle, M. A. Grace, and H. Halban, *Progress in Nuclear Physics* (Pergamon Press, London, 1957), Vol. 3, p. 63; M. J. Steenland and H. A. Tolhoek, *Progress in Low-Temperature Physics* (North-Holland Publishing Company, Amsterdam, 1957), Vol. 2, p. 292.

and the alignment:

$$p_2 = [1/I(2I-1)] [(\sum_i 3 \langle \Psi_i | I_z^2 | \Psi_i \rangle N_i / \sum_i N_i) - I(I+1)], \quad (2)$$

where N_i and Ψ_i are the population and the normalized wave function for the i^{th} the energy level. The polarization p_1 and the alignment p_2 are so defined as to lie between the limits ± 1 and to vanish for a random population distribution. For $I = \frac{1}{2}$, $p_2 = 0$, etc. The measurable quantities in solid-state and nuclear physics experiments with oriented nuclei depend in various ways upon the orientation parameters. For example, in magnetic resonance absorption the signal intensity is proportional to p_1 in loosely coupled systems, but in more complicated systems the signal may depend on a partial sum of Eq. (1). On the other hand, if the nuclei are radioactive and are emitting γ -rays or α -particles the angular distribution is a function of p_2, p_4, \dots . The angular distribution of β -particles may depend on p_1 and p_2 .

Generally speaking the dynamic nuclear orientation available may be of the order of $p_1 \sim h\nu/kT$, $p_2 \sim h\nu/kT$, \dots , where ν is the frequency of the applied rf field, h =Planck's constant, k =Boltzmann's constant, and T =absolute lattice temperature. Thus for $\nu \approx 3 \times 10^{10}$ cps, and $T \approx 1^\circ\text{K}$, appreciable orientations are obtainable. This dynamic nuclear orientation may be either transient or steady state, maintained by the dynamic equilibrium of the applied rf fields with the relaxation processes. In either case it is "dynamic" in contrast to the usual static orientation obtained in thermal equilibrium at very low temperatures by static hfs coupling.¹⁰

Before going into details we review in simple qualitative terms an idealized dynamic polarization experiment for a system of nuclear spins with $I = \frac{1}{2}$ in hyperfine coupling with electron spins with $S = \frac{1}{2}$. For example, consider a magnetically dilute crystal containing well-separated paramagnetic ions, each in an **I-S** type of hyperfine coupling with its own nucleus. If this crystal is placed in an external magnetic field H the energy levels will be as shown in Fig. 1, if we neglect the direct interaction of the nuclei with H in comparison to the hfs. The levels are approximately characterized by the electron magnetic quantum number $M = \langle S_z \rangle$ and the nuclear magnetic quantum number $m = \langle I_z \rangle$, as shown. Thermal processes induce transitions between each pair of levels, and after sufficient time the population of each level reaches its thermal equilibrium value given by the Boltzmann factor $\exp(-E_i/kT)$, Fig. 1(a). The energy spacings, Δ and δ , are in units of kT . We can think of the approach to thermal equilibrium as being due to relaxation transition probabilities which are greater for a downward transition than an upward one. We find for the static nuclear polarization $p_1 \approx \delta\Delta/4$, which is just the Rose-Gorter value.¹⁰ To obtain a dynamic polarization we may apply a sufficient rf

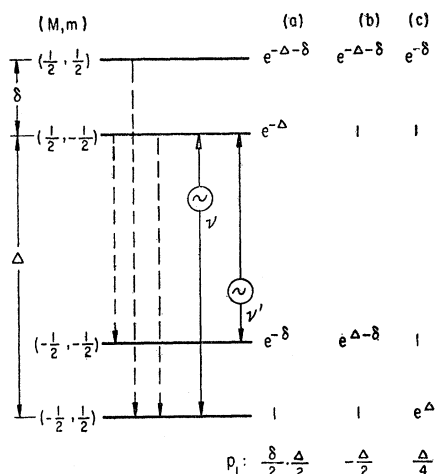


FIG. 1. Magnetic energy levels of a hyperfine system for $I=\frac{1}{2}$ and $S=\frac{1}{2}$, showing the relative (unnormalized) populations and nuclear polarization p_1 for: (a) thermal equilibrium; (b) dynamic equilibrium under the joint action of oscillator ν and relaxation transitions ($\Delta M=\pm 1$, $\Delta m=0$); (c) dynamic equilibrium under joint action of oscillator ν' and relaxation transitions ($\Delta M=\pm 1$, $\Delta m=0$) and ($\Delta M=\pm 1$, $\Delta m=\mp 1$).

field from a laboratory oscillator at the frequency ν to induce transitions between the two levels shown, corresponding to flipping the electron spins up and the nuclear spins down. Let us assume that even if this transition is forbidden in zero order, sufficient rf fields are available to induce this transition with a transition probability much greater than any of the relaxation transition probabilities. Since the induced emission transition probability is equal to that for absorption, this will essentially equalize the populations of these two levels, i.e., "saturate" them. The populations of the other two levels will be determined by the relaxation transition probabilities and we assume that the dominant ones are those of the classical paramagnetic relaxation, corresponding to $\Delta M=\pm 1$, $\Delta m=0$. The relaxation transitions will establish the steady-state population ratios:

$$N(\frac{1}{2}, -\frac{1}{2}) : N(-\frac{1}{2}, -\frac{1}{2}) = 1 : \exp(\Delta - \delta);$$

and

$$N(-\frac{1}{2}, \frac{1}{2}) : N(\frac{1}{2}, \frac{1}{2}) = 1 : \exp(-\Delta - \delta).$$

The resultant unnormalized populations are shown in Fig. 1(b). From Eq. (1) we find for the dynamic nuclear polarization $p_1 \approx -\Delta/2$, if $\Delta \ll 1$. This is larger than the static value by the factor $2/\delta \sim 10^2$, typically, at helium temperatures. On the other hand, if the assumed relaxation transitions are not dominant, but are greatly exceeded by ($\Delta m=\pm 1$, $\Delta M=0$) relaxation transitions, then the dynamic polarization is reduced to zero. Thus the all important question is, what are the relative relaxation rates, which we consider in detail in Sec. II.

We note that, alternately, if we apply the oscillator at the "allowed" frequency ν' between the $(\frac{1}{2}, -\frac{1}{2})$

and $(-\frac{1}{2}, -\frac{1}{2})$ levels and assume the additional cross relaxation transitions ($\Delta M=\pm 1$, $\Delta m=\mp 1$), we can produce the populations of Fig. 1(c), leading to a dynamic nuclear polarization $p_1 \approx \Delta/4$. This second method, which we will call dynamic polarization by saturation of allowed transitions, is a direct generalization⁴ of Overhauser's original suggestion and is to be contrasted to the first method in the preceding paragraph, which we will call dynamic polarization by forbidden transitions. The two methods are indeed very closely related and the relative advantages will be discussed in Sec. II. At this point we merely note that the essential feature of both methods is a simultaneous flipping of an electron spin and a nuclear spin. In the second method it is the cross relaxation transitions which flip the nuclei and give rise to a polarization; in the first method it is the applied rf fields which directly flip the nuclei, producing a polarization.

Our use throughout this paper of the term forbidden transition to denote an rf-induced simultaneous flip of an electron and a nuclear spin is admittedly a poor notation, since the transition probability may, in some cases, be comparable to that for the usual allowed transitions $\Delta M=\pm 1$, $\Delta m=0$. Furthermore, as Abragam¹¹ has pointed out, these transitions may be induced by ultrasonic waves, in which case they are not relatively forbidden.

It should be pointed out that a low-frequency prototype of dynamic nuclear orientation in solids was first performed by Pound¹² some time ago, essentially the only difference being that instead of an electron-nucleus coupled system he used a pure nuclear system with unequally spaced levels due to both nuclear Zeeman and quadrupole interactions. In his system, $(\Delta/\delta) \sim 2$ and the dynamic nuclear orientation was only about twice the static value, but still readily detectable by magnetic resonance.

For detailed considerations we adopt the spin Hamiltonian of Abragam and Pryce¹³ for a system of electron spins and nuclear spins in a crystal in a magnetic field H at such low temperature that only the lowest electronic state is significantly populated and has a degeneracy $2S+1$:

$$\mathcal{H} = \sum_{k,l=1}^3 (H_k \beta g_{kl} S_l + S_k A_{kl} I_l + I_k P_{kl} I_l) + g_n \beta \mathbf{H} \cdot \mathbf{I} + \mathcal{H}_c. \quad (3)$$

The terms represent, consecutively, the electronic Zeeman, magnetic hyperfine, nuclear electric quadrupole, nuclear Zeeman, and electronic crystal field interactions. It is assumed that the crystal is magnetically dilute. For the present we take $\mathcal{H}_c=0$; the more

¹¹ A. Abragam and W. G. Proctor, *Compt. rend.* **246**, 2253 (1958).

¹² R. V. Pound, *Phys. Rev.* **79**, 685 (1950).

¹³ A. Abragam and M. H. L. Pryce, *Proc. Roy. Soc. (London)* **A205**, 135 (1951).

general case of $\mathcal{H}_c \neq 0$ will be treated in a later paper⁹ on Mn.^{52,54}

Of the many possible systems of physical interest we choose to discuss in detail in Sec. II the case of diluted paramagnetic ions in a single crystal, each in relatively strong hfs coupling with its own nucleus. This system is particularly useful for dynamic orientation experiments with minute quantities of radionuclei paramagnetic atoms to determine their nuclear moments. We make the simplifying and not too restrictive assumptions that a set of crystal coordinates (x', y', z') may be chosen which are the principal axes of all the tensors in Eq. (3). Only the diagonal terms remain and may be rewritten, assuming axial symmetry about z' , as:

$$\begin{aligned} {}_0\mathcal{H} = & g_{11}\beta H_{z'}S_{z'} + g_{\perp}\beta(H_{x'}S_{x'} + H_{y'}S_{y'}) + AS_{z'}I_{z'} \\ & + B(S_{x'}I_{x'} + S_{y'}I_{y'}) + P[I_{z'}^2 - I(I+1)/3] \\ & + g_n\beta(H_{x'}I_{x'} + H_{y'}I_{y'} + H_{z'}I_{z'}). \end{aligned} \quad (4)$$

Here g_{11} and g_{\perp} are the electronic spectroscopic splitting factors along and perpendicular, respectively, to the z' axis; S =effective electron spin; I =nuclear spin; $A=A_{z'z'}$ and $B=A_{x'x'}=A_{y'y'}$ are the magnetic hfs coupling constants (in ergs) parallel and perpendicular respectively, to the z' axis and are proportional, for a given ion, to g_n ; $g_n=\mu_n/I$ =nuclear g factor, where μ_n is the nuclear magnetic moment in Bohr magnetons; β =Bohr magneton; P is the nuclear quadrupole coupling constant and is rarely large enough to be detected. We have taken $\mathbf{u} = -g\beta\mathbf{S}$ and $\mathbf{v} = -g_n\beta\mathbf{I}$ in the definition of the algebraic sign of the g factors. In Sec. II, following Abragam,⁴ we consider ${}_0\mathcal{H}$ of Eq. (4) to be subject to the perturbations ${}_r\mathcal{H}(t) + {}_T\mathcal{H}(t)$, where ${}_r\mathcal{H}(t)$ is a time-dependent perturbation on ${}_0\mathcal{H}$ due to applied rf fields and ${}_T\mathcal{H}(t)$ is a random time-dependent perturbation representing thermal relaxation interactions of the spin system with the lattice, considered as a "bath." The various transitions are discussed and calculations are made for the polarization p_1 and the alignment p_2 to be expected upon saturation of various allowed and forbidden transitions.

In Sec. III we similarly consider briefly a system of nuclear spins in weak long-range dipolar coupling with electron spins, particularly from the viewpoint of dynamic orientation of radionuclei of diamagnetic atoms.

In Sec. IV are given explicit expressions for the γ -ray anisotropy of dynamically oriented radionuclei and in Sec. V a brief comparison is made with the general experimental results.^{8,9}

II. PARAMAGNETIC IONS IN STRONG hfs COUPLING

A. rf-Induced Transition Probabilities

1. Magnetic hfs

We introduce a set of laboratory coordinates (x, y, z) in which the applied dc field $H\|z$, and transform the

spin Hamiltonian Eq. (4) to these coordinates for two cases of crystal orientation: (1) the parallel (\parallel) case, i.e., for $z'\|z$, $x'\|x$, $y'\|y$; and (2) the perpendicular (\perp) case, i.e., for $z'\|x$, $x'\|z$, $y'\|y$. Dropping for the moment the term in P and introducing the raising and lowering operators $I_{\pm}=I_x \pm iI_y$, $S_{\pm}=S_x \pm iS_y$ we obtain

$${}_0\mathcal{H}_{\parallel} = g_{11}\beta HS_z + AI_zS_z + \frac{1}{2}B(S_-I_+ + S_+I_-) + g_n\beta HI_z, \quad (5)$$

$$\begin{aligned} {}_0\mathcal{H}_{\perp} = & g_{\perp}\beta HS_z + BI_zS_z + \frac{1}{4}(A+B)(S_-I_+ + S_+I_-) \\ & + \frac{1}{4}(A-B)(S_-I_- + S_+I_+) + g_n\beta HI_z. \end{aligned} \quad (6)$$

These matrix elements will be useful:

$$\langle Mm | S_{\pm}I_{\mp} | M'm' \rangle = R_{\pm} r_{\mp} \delta_{M, M' \pm 1} \delta_{m, m' \mp 1}, \quad (7)$$

$$\langle Mm | S_{\pm}I_{\pm} | M'm' \rangle = R_{\pm} r_{\pm} \delta_{M, M' \pm 1} \delta_{m, m' \pm 1}, \quad (8a)$$

where

$$\begin{aligned} r_{\pm} &= [(I \pm m)(I \mp m + 1)]^{\frac{1}{2}}, \\ R_{\pm} &= [(S \pm M)(S \mp M + 1)]^{\frac{1}{2}}. \end{aligned} \quad (8b)$$

Usually we will have (electron Zeeman energy) \gg (magnetic hfs energy) \gg nuclear Zeeman energy, in which case the energies are found from a second-order perturbation calculation,

$$\begin{aligned} E_{11} = & g_{11}\beta HM + AMm + (B^2/2g_{11}\beta H)\{[I(I+1) - m^2]M \\ & - m[S(S+1) - M^2]\} + g_n\beta Hm, \end{aligned} \quad (9)$$

$$\begin{aligned} E_{\perp} = & g_{\perp}\beta HM + BMm + (A^2 + B^2/4g_{\perp}\beta H) \\ & \times [I(I+1) - m^2]M - (AB/2g_{\perp}\beta H) \\ & \times [S(S+1) - M^2]m + g_n\beta Hm. \end{aligned} \quad (10)$$

We label the levels by the zero order quantum numbers (M, m), where $M=\langle S_z \rangle$, $m=\langle I_z \rangle$. Transitions between these levels are usually induced by applying suitable rf fields at a fixed frequency $\nu_0 \equiv g\beta H_0/h$ and varying the magnetic field H . For example, for $S=\frac{1}{2}$, allowed transitions $(\frac{1}{2}, m) \leftrightarrow (-\frac{1}{2}, m)$ occur at these fields, approximately,

$$H_{11} = H_0 - \frac{Am}{g_{11}\beta} - \left(\frac{B^2}{2g_{11}^2\beta^2 H_0} \right) [I(I+1) - m^2], \quad \text{for } z'\|H, \quad (11)$$

$$H_{\perp} = H_0 - \frac{Bm}{g_{\perp}\beta} - \left(\frac{A^2 + B^2}{4g_{\perp}^2\beta^2 H_0} \right) [I(I+1) - m^2], \quad \text{for } z'\perp H. \quad (12)$$

So-called forbidden transitions $(\frac{1}{2}, m) \leftrightarrow (-\frac{1}{2}, m \pm 1)$ occur at these fields, approximately,

$$\begin{aligned} H_{11} = & H_0 - \frac{A}{g_{11}\beta} (m \pm \frac{1}{2}) - \left(\frac{B^2}{2g_{11}^2\beta^2 H_0} \right) [I(I+1) \\ & - m(m \pm 1) \pm \frac{1}{2} - \frac{1}{2}] \pm H_0 g_n / g_{11}, \quad \text{for } z'\|H, \end{aligned} \quad (13)$$

$$H_1 = H_0 - \frac{B}{g_1 \beta} (m \pm \frac{1}{2}) - \left(\frac{A^2 + B^2}{4g_1^2 \beta^2 H_0} \right) [I(I+1) - m(m \pm 1) + \frac{1}{2}] \pm \frac{AB}{4g_1^2 \beta^2 H_0} \pm H_0 g_n / g_1, \text{ for } z' \perp H. \quad (14)$$

We find the approximate wave functions of these magnetic hfs levels by taking zero order functions $\psi^0(M, m)$ corresponding to an electron and a nucleus in a huge magnetic field. The hfs term admixes these slightly and a first order perturbation calculation yields, for $z' \parallel H$,

$$\psi_{11}(M, m) = q_0 \psi^0(M, m) + q_- \psi^0(M+1, m-1) + q_+ \psi^0(M-1, m+1), \quad (15a)$$

where

$$q_0^2 + q_-^2 + q_+^2 = 1,$$

and

$$q_{\pm} = \pm BR_{\pm} r_{\pm} / 2g_{11} \beta H. \quad (15b)$$

For $z' \perp H$,

$$\psi_1(M, m) = a_0 \psi^0(M, m) + a_+ \psi^0(M-1, m+1) + a_- \psi^0(M+1, m-1) + b_+ \psi^0(M+1, m+1) + b_- \psi^0(M-1, m-1), \quad (15c)$$

where

$$a_0^2 + a_+^2 + a_-^2 + b_+^2 + b_-^2 = 1,$$

and

$$a_{\pm} = \pm (A+B) R_{\pm} r_{\pm} / 4g_1 \beta H, \quad (15d)$$

$$b_{\pm} = \mp (A-B) R_{\pm} r_{\pm} / 4g_1 \beta H. \quad (15e)$$

At this point we note that the spin Hamiltonian, Eqs. (5) and (6), and the above discussion applies, strictly speaking, to a single isolated electron-nucleus hfs-coupled pair. We are actually concerned with a system consisting of a large number, $N \sim 10^{15}$, of such pairs, still more or less isolated from each other but coupled to a crystal lattice in which they are imbedded. We use the usual perturbation methods and optical concepts,^{4,14,15} and accordingly we consider a *typical pair* to be described by the foregoing spin Hamiltonian, energies, etc., and distribute the N pairs over the energy levels of a single pair.

The action of an applied rf field \mathbf{H}_1 with components $H_{1x} \cos \omega t$, $H_{1y} \cos \omega t$, $H_{1z} \cos \omega t$ will be found by introducing a time-dependent perturbation $r_{\text{rf}} \mathcal{C}(t) = r_{\text{rf}} \mathcal{C} \cos \omega t$. We take

$$r_{\text{rf}} \mathcal{C}_{11} = g_{11} \beta H_{1x} S_z + \frac{1}{2} g_1 \beta [(H_{1x} - iH_{1y}) S_+ + (H_{1x} + iH_{1y}) S_-], \text{ for } z' \parallel H, \quad (16)$$

$$r_{\text{rf}} \mathcal{C}_1 = g_1 \beta H_{1x} S_z + \frac{1}{2} \beta [(H_{1x} g_{11} - iH_{1y} g_1) S_+ + (H_{1x} g_{11} + iH_{1y} g_1) S_-], \text{ for } z' \perp H, \quad (17)$$

as perturbations on Eq. (5) and on Eq. (6), respectively;

¹⁴ N. Bloembergen, E. M. Purcell, and R. V. Pound, Phys. Rev. **73**, 679 (1948).

¹⁵ J. P. Lloyd and G. E. Pake, Phys. Rev. **94**, 579 (1954).

terms in g_n are quite negligible. Here \mathbf{H}_1 may be a standing wave field in a microwave cavity and H_{1z} represents the component parallel to the dc field. Let the system be initially in a state $\psi(M, m)$ and let $r_{\text{rf}} \mathcal{C}(t)$ be turned on at time $t=0$. Then by the usual first order time-dependent perturbation theory the probability that the system will be found at time $t=\tau$ in the state $\psi'(M', m')$ is¹⁶

$$|a(\tau)|^2 = \hbar^{-2} \left| \int_0^\tau \langle \psi' | r_{\text{rf}} \mathcal{C}(t) | \psi \rangle \exp(i\omega' t) dt \right|^2, \quad (18)$$

where $\omega' = (E - E')/\hbar$. On considering the time-dependent factors in Eq. (18), we obtain

$$|a(\tau)|^2 \propto (\omega' - \omega)^{-2} \sin^2[\tau(\omega' - \omega)/2]. \quad (19)$$

Now in the total system, i.e., N spin pairs, we may expect a distribution of values of E and E' , and we now assume a continuous distribution of states peaked about E and also about E' , in correspondence with a finite sample line width characterized by the line shape function $g(\nu)$, so normalized that $\int_0^\infty g(\nu) d\nu = 1$. If Eq. (19) is averaged over $g(\nu)$ for a time $\tau \gg T_2$, where T_2 is the inverse line width $(\Delta\omega)^{-1}$ one obtains $\tau g(\nu)/4$. Thus one obtains a transition probability per second averaged over the whole system,

$$W(M, m \rightarrow M', m') = \overline{|a(\tau)|^2} / \tau = g(\nu) (2\hbar)^{-2} \times |\langle Mm | r_{\text{rf}} \mathcal{C} | M'm' \rangle|^2 \text{ sec}^{-1}, \quad (20)$$

which will be the same as $W(M', m' \rightarrow M, m)$, since $r_{\text{rf}} \mathcal{C}$ is Hermitian.

We evaluate Eq. (20) for the crystalline axis $z' \parallel H$ by using Eq. (16) and the wave functions of Eq. (15a), assuming $q_0 \approx 1$, $q_{\pm} \ll 1$ and neglecting terms of order $(q_+ q_-)^2$, and find the transition probabilities

$$W_1(M, m \rightarrow M \pm 1, m) = C g_1^2 (H_{1x}^2 + H_{1y}^2) R_{\mp}^2 / 4 \text{ sec}^{-1}, \quad (21)$$

$$W_2(M, m \rightarrow M \pm 1, m \mp 1) = C g_{11}^2 H_{1x}^2 \alpha^2 R_{\mp}^2 r_{\pm}^2 \text{ sec}^{-1}, \quad (22)$$

$$\bar{W}_4(M, m \rightarrow M, m \mp 1) = C g_1^2 (H_{1x}^2 + H_{1y}^2) \alpha^2 r_{\pm}^2 M^2 \text{ sec}^{-1} \quad (23)$$

where $C = g(\nu) \beta^2 / 4\hbar^2$, $\alpha = B / 2g_{11} \beta H$, and R_{\pm} , r_{\pm} are given by Eq. (8b). For $z' \perp H$ we use Eqs. (17) and (15c) to obtain similarly

$$W_1(M, m \rightarrow M \pm 1, m) = C (g_{11}^2 H_{1x}^2 + g_1^2 H_{1y}^2) R_{\mp}^2 / 4 \text{ sec}^{-1}, \quad (24)$$

$$W_2(M, m \rightarrow M \pm 1, m \mp 1) = C g_1^2 H_{1x}^2 \gamma_{\pm}^2 R_{\mp}^2 r_{\pm}^2 \text{ sec}^{-1}, \quad (25)$$

¹⁶ L. I. Schiff, *Quantum Mechanics* (McGraw-Hill Book Company, Inc., New York, 1949), Chap. VIII.

$$W_3(M, m \rightarrow M \pm 1, m \pm 1) = C g_1^2 H_{1z}^2 \gamma_{\mp}^2 R_{\mp}^2 \sec^{-1}, \quad (26)$$

$$W_4(M, m \rightarrow M, m \mp 1) = C [g_{11}^2 H_{1x}^2 (\gamma_+ + \gamma_-)^2 + g_1^2 H_{1y}^2 (\gamma_+ - \gamma_-)^2] r_{\pm}^2 M^2, \quad (27)$$

where $\gamma_{\pm} = (A \pm B)/4g_1\beta H$.

The transitions, Eq. (21)–Eq. (27), are shown schematically in Fig. 2 for $S = \frac{1}{2}$ and $I = 1$, arbitrarily chosen. W_1 corresponds to the usual allowed transitions induced by the perpendicular rf field component. Transitions W_3 and W_2 , forbidden in zero order, correspond to a simultaneous flipping of electron and nuclear spins in the same and opposite directions, respectively, and are of interest in dynamic orientation; they are induced by the parallel rf field component and are weaker than W_1 by the order $\alpha^2 \sim \gamma^2 \sim 2 \times 10^{-3}$, typically, but are nevertheless often observed in paramagnetic resonance spectra.¹⁷ For $z' \perp H$ we note that $W_2/W_3 = (A+B)^2/(A-B)^2$, which becomes unity if $|A|$ is either much larger or much smaller than $|B|$. For $z' \parallel H$, $W_3 = 0$. Transitions W_4 correspond to low-frequency transitions, which are useful in double-resonance experiments.¹⁸

The spin Hamiltonian, Eq. (4), and the above discussion apply to paramagnetic ions in crystals which have at least a double degeneracy in the lowest state. By Kramer's theorem all ions with an odd number of unpaired electrons have this degeneracy. An even number of unpaired electrons requires individual consideration in each case, but for some cases (e.g., Ni^{2+} , Ho^{3+}) an effective spin Hamiltonian of the form of Eq. (4) is valid and the above discussion applies. However other cases (e.g., Fe^{2+} , Pr^{3+} , Tb^{3+}) are approximately represented by a spin Hamiltonian in the crystal coordinates ($x'y'z'$) of the form¹⁹:

$$3\mathcal{C} = g_{11}\beta S_{z'}H \cos\theta + A\mathbf{I} \cdot \mathbf{S}_{z'} + \Delta_{x'}S_{x'} + \Delta_{y'}S_{y'}, \quad (28)$$

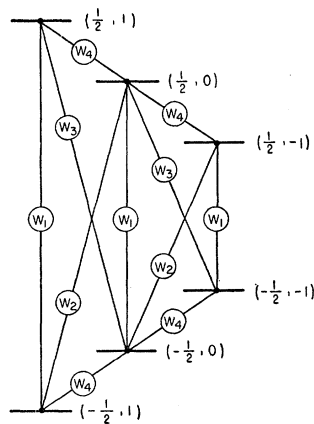


FIG. 2. Rf-induced transitions, Eq. (21)–Eq. (27), for an hfs system with $S = \frac{1}{2}$, $I = 1$. The levels are characterized by (M, m) .

where θ is the angle between z' and the dc field \mathbf{H} , and the small terms $\Delta_{x'}$, $\Delta_{y'}$ probably arise from a random distribution of crystal fields of low symmetry. An applied rf field has no matrix elements between the zero order wave functions $\psi^0(M, m)$, since $g_1 = 0$. The Δ terms admix the states so that $\psi(M, m) = a\psi^0(M, m) + b_{\pm}\psi^0(M \pm 1, m)$, and the rf field component H_{1z} induces transitions of type W_1 in first order. However, dynamic nuclear orientation by saturation of transitions of type W_2 or W_3 will not be practicable in this case, since these transitions are highly forbidden, being induced only by the small (previously neglected) term $g_n\beta\mathbf{H}_1 \cdot \mathbf{I} \cos\omega t$.

2. Nuclear Electric Quadrupole Interactions

Forbidden transitions obeying the selection rules of W_2 and W_3 may also be obtained through a mixing of the zero order functions by the quadrupole term P in Eq. (4), as discussed in detail by Bleaney.²⁰ To review this case we take a spin Hamiltonian in the laboratory coordinates:

$$3\mathcal{C} = g\beta H S_z + A\mathbf{I} \cdot \mathbf{S} + P[(I_z \cos\theta + I_x \sin\theta)^2 - I(I+1)/3], \quad (29)$$

where θ is the angle between z and the crystalline axis z' , with $y \parallel y'$, and we have assumed isotropic g and A tensors. Let $P \lesssim A$. Neglecting terms in $A/g\beta H$, the first order wave functions will be:

$$\begin{aligned} \psi(M, m) = & p_0\psi^0(M, m) + p_+\psi^0(M, m+1) \\ & + p_-\psi^0(M, m-1) \\ & + s_+\psi^0(M, m+2) + s_-\psi^0(M, m-2), \end{aligned} \quad (30a)$$

where

$$p_{\pm} = \mp P \sin\theta \cos\theta (2m \pm 1) r_{\pm} / 2AM, \quad (30b)$$

$$s_{\pm} = \mp P \sin^2\theta (I \pm m \pm 2)(I \mp m - 1) r_{\mp} / 8AM. \quad (30c)$$

The quadrupole interaction adds to the energy, Eqs. (9) and (10), this term:

$$E_p = P[(\frac{3}{2}) \cos^2\theta - \frac{1}{2}][m^2 - I(I+1)/3]. \quad (31)$$

An applied rf field, represented by a perturbation like that of Eq. (16), induces the usual allowed transitions given by W_1 of Eq. (21). In addition, the following forbidden transitions are induced:

$$W_2(M, m \rightarrow M \pm 1, m \mp 1) = W_1 p_{\mp}^2 (M \pm 1)^{-2} \sec^{-1}, \quad (32a)$$

$$W_3(M, m \rightarrow M \pm 1, m \pm 1) = W_1 p_{\pm}^2 (M \pm 1)^{-2} \sec^{-1}, \quad (32b)$$

$$W_5(M, m \rightarrow M \pm 1, m \mp 2) = W_1 s_{\mp}^2 (M \pm 1)^{-2} \sec^{-1}, \quad (33a)$$

$$W_6(M, m \rightarrow M \pm 1, m \pm 2) = W_1 s_{\pm}^2 (M \pm 1)^{-2} \sec^{-1}. \quad (33b)$$

¹⁷ See, for example, B. Bleaney, H. E. D. Scovil, and R. S. Trenan, Proc. Roy. Soc. (London) **A223**, 15 (1954).

¹⁸ G. Feher, Phys. Rev. **103**, 834 (1956).

¹⁹ J. M. Baker and B. Bleaney, Proc. Roy. Soc. (London) **A245**, 156 (1958).

²⁰ B. Bleaney, Phil. Mag. **42**, 441 (1951).

The positions of the allowed transitions W_1 are unchanged by the addition of E_p , Eq. (31). However the transitions W_2 and W_3 above are shifted in position and a term $P(1 \pm 2m)[(\frac{3}{2}) \cos^2 \theta - \frac{1}{2}]/g\beta$ must be added to Eqs. (13) or (14).

We note that in the quadrupole case W_2 and W_3 , Eqs. (32a) and (32b), are weaker than W_1 by the factor $\sim (P/A)^2$, which in some cases will be considerably larger than the factor $(A/g\beta H)^2$ for the magnetic hfs case of Eq. (22). For example, all the transitions Eq. (32) and Eq. (33) have been observed in the paramagnetic resonance spectra of Cu^{2+21} and U^{3+22} with the intensities only about one order of magnitude less than the main transitions. There is no evidence in the resonance spectra of most paramagnetic ions, however, of an appreciable quadrupole term, i.e., the data are consistent with $P \lesssim A/50$, typically. We note nevertheless that because of random lattice distortions, etc., there may exist in some cases an appreciable mean square quadrupole interaction $\langle P^2 \rangle_{\text{av}}$, with a vanishing average value of P . Thus the average positions of the transitions W_2 and W_3 would be given by Eqs. (13) and (14), but the intensities by Eqs. (32a) and (32b).

We generally conclude that quadrupole interactions are an important source of matrix elements for forbidden transitions useful in dynamic nuclear orientation.

B. Relaxation Transitions

We make no proper attempt here to calculate transition probabilities due to thermal processes. We try, instead, to merely represent the various complex relaxation interactions by simple and approximate Hamiltonians of arbitrary magnitude. These are considered as time-dependent perturbations on the spin Hamiltonian, Eq. (5) or (6), and relaxation transition probabilities per second are calculated, the object being to find the selection rules and the relative transition probabilities for certain simple assumptions.

We assume that the most important relaxation interactions may be approximately represented by

$$\begin{aligned} \tau \mathcal{H}(t) = \sum_{k,l} [S_k \beta g_{kl} H_l'(t) + S_k \beta \lambda_{kl}(t) H_l + I_k \beta g_n H_l''(t) \\ + S_k F_{kl}(t) I_l + I_k p_{kl}(t) I_l + S_k d_{kl}(t) S_l]. \quad (34) \end{aligned}$$

The first and second terms represent the electron spin-lattice interaction where $H_l'(t)$ is an equivalent fluctuating magnetic-field component due to thermal agitation of the lattice, and $\lambda_{kl}(t)$ is a fluctuating component of the g tensor due to thermal modulation of the spin-orbit coupling. The third term represents the direct nuclear-lattice interaction and will usually be quite negligible. The fourth term represents the thermal modulation of the magnetic hfs interaction, where

²¹ B. Bleaney, K. D. Bowers, and D. J. E. Ingram, Proc. Roy. Soc. (London) A228, 147 (1955).

²² P. B. Dorain, C. A. Hutchison, Jr., and E. Wong, Phys. Rev. 105, 1307 (1957).

$F_{kl}(t)$ is a fluctuating component of the A tensor. The fifth and sixth terms similarly represent the fluctuations in the nuclear electric quadrupole interaction and in the crystal field interaction, respectively.

We write Eq. (34) as $\tau \mathcal{H}(t) = \sum_n \tau \mathcal{H}_n(t)$ and assume that each of the time variables has a broad and smooth frequency spectrum so that a typical term in Eq. (34) [e.g., $S_x F_{xz}(t) I_z$] may be represented by $\tau \mathcal{H}_n(t) = \sum_{\nu} \tau \mathcal{H}_n^{\nu}(t)$ where $\tau \mathcal{H}_n^{\nu}(t) = b_n^{\nu} Q_n \cos[2\pi \nu t + \varphi_n^{\nu}(t)]$ is the Fourier component at frequency ν ; Q_n is a spin operator (e.g., $S_x I_z$). We assume that the phase $\varphi_n^{\nu}(t)$ is a random variable such that the correlation function $\langle \varphi_n^{\nu}(t) \varphi_n^{\nu}(t+\tau) \rangle_{\text{av}} = f_n^{\nu}(\tau)$ is sharply peaked about $\tau=0$ with a width $\sim \tau_n^{\nu}$ = self-correlation time. Then in a way similar to that for Eq. (20) we find an average transition probability per second due to $\tau \mathcal{H}_n(t)$ for times $\tau \gg \tau_n^{\nu}$:

$$\begin{aligned} W_n(M, m \rightarrow M', m') = \sum_{\nu} |a_n^{\nu}(\tau)|^2 / \tau \\ = (2\hbar)^{-2} J_n(\nu') | \langle Mm | Q_n | M'm' \rangle |^2, \quad (35) \end{aligned}$$

where $\nu' = (E - E')/\hbar$, and $J_n(\nu') \Delta \nu = |b_n^{\nu'}|^2 =$ mean squared fluctuation energy density between ν' and $\nu' + \Delta \nu$ due to the term $\tau \mathcal{H}_n(t)$ alone. Other terms with the same matrix elements, i.e., the same frequency ν' , will simply add to this if we assume, for the moment, that the cross terms vanish because of incoherence, i.e., $\tau \gg \tau_{nm}^{\nu} =$ cross-correlation time, defined by $\langle \varphi_n^{\nu}(t) \times \varphi_m^{\nu'}(t + \tau_{nm}^{\nu}) \rangle_{\text{av}} \approx \frac{1}{2} \langle \varphi_n^{\nu}(0) \varphi_m^{\nu'}(0) \rangle_{\text{av}}$.

As an example we consider separately the magnetic hfs relaxation term, expanding in the laboratory coordinates the component at frequency ν :

$$\begin{aligned} \sum_{k,l} S_k F_{kl} I_l = G S_z I_z + B_- S_- I_+ + B_+ S_+ I_- + C_- S_+ I_+ \\ + C_+ S_- I_- + D_- S_+ I_z + D_+ S_- I_z \\ + E_- S_z I_+ + E_+ S_z I_-, \quad (36) \end{aligned}$$

where $4B_{\pm} = [F_{xx}^{\nu} + F_{yy}^{\nu} \pm i(F_{xy}^{\nu} - F_{yx}^{\nu})]$, $4C_{\pm} = [F_{xx}^{\nu} - F_{yy}^{\nu} \pm i(F_{xy}^{\nu} + F_{yx}^{\nu})]$, $2D_{\pm} = [F_{xz}^{\nu} \pm iF_{yz}^{\nu}]$, $2E_{\pm} = [F_{zx}^{\nu} \pm iF_{zy}^{\nu}]$, $G = F_{zz}^{\nu}$. Using zero order functions $\psi^0(M, m)$ we find the following transition probabilities per second for the most general assumption that the nine components $F_{kl}^{\nu}(t)$ are all independent and completely uncorrelated:

$$\begin{aligned} \tau W_1(M, m \rightarrow M \pm 1, m) \\ = [J_{xz}(\nu_1) + J_{yz}(\nu_1)] R_{\mp}^2 m^2 / 16 \hbar^2, \quad (37a) \end{aligned}$$

$$\begin{aligned} \tau W_2(M, m \rightarrow M \pm 1, m \mp 1) \\ = [J_{xz}(\nu_2) + J_{yz}(\nu_2) + J_{xy}(\nu_2) \\ + J_{yx}(\nu_2)] R_{\mp}^2 r_{\pm}^2 / 64 \hbar^2, \quad (37b) \end{aligned}$$

$$\begin{aligned} \tau W_3(M, m \rightarrow M \pm 1, m \pm 1) \\ = [J_{xz}(\nu_3) + J_{yz}(\nu_3) + J_{xy}(\nu_3) \\ + J_{yx}(\nu_3)] R_{\mp}^2 r_{\mp}^2 / 64 \hbar^2, \quad (37c) \end{aligned}$$

$$\begin{aligned} \tau W_4(M, m \rightarrow M, m \mp 1) \\ = [J_{zx}(\nu_4) + J_{zy}(\nu_4)] M^2 r_{\pm}^2 / 16 \hbar^2. \quad (37d) \end{aligned}$$

Here we have introduced the spectral densities $J_{xx}(\nu_1) = |F_{xx\nu_1}|^2 \Delta\nu$, etc., where $\nu_1 h$ is the energy difference for transitions W_1 , etc.

From Eqs. (37b) and (37c) we note that if we assume a reasonably flat spectral density, $J_{xx}(\nu_2) \approx J_{xx}(\nu_3)$, then $\tau W_3 = \tau W_2$, i.e., the probability that an electron and a nuclear spin be simultaneously flipped in the same direction is equal to the probability that they be flipped simultaneously in opposite directions. This could cause the dynamic nuclear orientation obtained by saturating allowed transitions to vanish in first order, as shown below. On the other hand, if we assume the other extreme case, namely, that the nine components $F_{kl}^\nu(t)$ are completely coherent, $\tau \ll \tau_{nm}^\nu$, then τW_1 and τW_4 are unchanged but cross terms add to τW_2 and subtract from τW_3 , so that they are no longer equal.

Furthermore in many cases, e.g., when \mathbf{S} is a real spin vector,²³ the A tensor is symmetric and we expect the F tensor to be likewise: $F_{kl}^\nu(t) = F_{lk}^\nu(t)$. This assumption does not change τW_1 or τW_4 but the bracketed factor in Eq. (37c) becomes $[J_{xx} + J_{yy} + 4J_{xy}]$ and in Eq. (37b) it becomes $[J_{xx} + J_{yy}]$, again making $\tau W_2 \neq \tau W_3$, unless the off-diagonal term J_{xy} is negligible. Finally if we assume complete coherence, $F_{xx} = F_{yy}$, and vanishing off-diagonal terms ($F_{xy} = 0$, etc.), then $\tau W_2 \neq 0$, $\tau W_1 = \tau W_3 = \tau W_4 = 0$, which is the special case previously considered by Abragam.⁴ Consideration of a definite model is necessary for a more specific estimate of the transition probabilities but we generally conclude from this discussion that τW_1 , τW_2 , τW_3 , τW_4 may all be of the same order of magnitude, perhaps even $\tau W_2 = \tau W_3$ in some cases, but only in special cases does $\tau W_3 = 0$.

Similar consideration of the first two terms of Eq. (34) show that they will produce relaxation transition probabilities $\tau W'$ essentially given by Eq. (21)–Eq. (27) if we replace C by $\beta^2/4\hbar^2$ and $g_1^2 H_{1x}^2$ by $K_x(\nu)$, etc., where $K_x(\nu)\Delta\nu$ is a component of the fluctuating magnetic energy density between ν and $\nu + \Delta\nu$. The transition probability $\tau W_1'$ corresponds to the classical paramagnetic relaxation and will probably be dominant, particularly for paramagnetic ions in hydrated crystals. The transition $\tau W_2'$ is weaker by the order $(B/g\beta H)^2$ and must be added to τW_2 of Eq. (37b), which may dominate it at high fields but not at low fields. For $z \parallel H$, $\tau W_3' = 0$ but for $z' \perp H$, $\tau W_3'$ may be an important addition to τW_3 of Eq. (37c).

The nuclear quadrupole term in Eq. (36) may be an important process in some cases. Even if the static tensor P_{kl} vanishes, e.g., because of cubic symmetry, the fluctuating tensor $p_{kl}(t)$ does not necessarily do so. This term induces relaxation transitions of the types $W(M, m \rightarrow M, m \pm 1)$ and $W(M, m \rightarrow M, m \pm 2)$ and could even be the dominant process if P_{kl} is unusually large ($\sim 0.03 \text{ cm}^{-1}$).

²³ B. Bleaney and M. C. M. O'Brien, Proc. Phys. Soc. (London) **B69**, 1216 (1956).

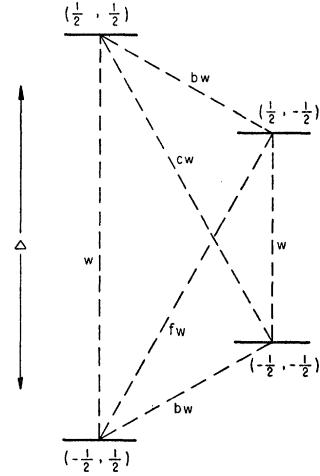


FIG. 3. Relaxation transitions for an hfs system with $I = \frac{1}{2}$, $S = \frac{1}{2}$. The levels are characterized by (M, m) .

The crystal field splitting term $d_{kl}(t)$ may also be important particularly if the static term D_{kl} is large. In zero order it induces relaxation transitions of the types $W(M, m \rightarrow M \pm 1, m)$ and $W(M, m \rightarrow M \pm 2, m)$. In first order, transitions of the type $W(M, m \rightarrow M \pm 1, m \mp 1)$ may also be induced, weaker by $(B/g\beta H)^2$.

We summarize this section by means of Fig. 3, which represents schematically for the case $I = \frac{1}{2}$, $S = \frac{1}{2}$ the various relaxation transition probabilities. For example, $w = \sum \tau W_1$ is the sum of all the transition probabilities per second for the transition $(M, m \rightarrow M \pm 1, m)$ due to the various terms in Eq. (34); bw is a similar quantity for $(M, m \rightarrow M, m \pm 1)$, where b is a dimensionless factor; etc. In view of the above discussion we consider that it will not be unrealistic to suppose that c , b , and f may have almost any values between zero and unity, approximately. In the following section we calculate dynamic populations for several "typical" cases.

C. Populations, Polarization and Alignment

We have $N \sim 10^{15}$ electron-nuclear hfs coupled pairs to be distributed over a closed group of $n = (2I + 1)(2S + 1)$ energy levels; let N_i be the population of the i th level. Under the simultaneous action of applied rf fields and relaxation processes the populations are given by the rate equations

$$dN_i/dt = \sum_{j \neq i}^n [N_j(W_{ji} + U_{ji}) - N_i(W_{ij} + U_{ij})], \quad i = 1, 2, \dots, n. \quad (38)$$

Here $W_{ji} = W_{ij} = W(M, m \leftrightarrow M', m')$ is the rf-oscillator-induced transition probability per second between ψ_i and ψ_j ; $U_{ji} = w_{ji}\rho_i$ is the effective relaxation transition probability per second from ψ_j to ψ_i and $U_{ij} = w_{ij}\rho_j$ is the effective relaxation transition probability per second from ψ_i to ψ_j , where $\rho_i = \exp(-E_i/kT)$ and $w_{ij} = w_{ji}$ is the total transition probability per second

due to all thermal perturbations as calculated in *B* above. The Boltzmann factors ρ_i, ρ_j are introduced to reflect the fact that the relaxation transitions are the result of thermal processes and, in the absence of rf fields, yield after sufficient time the steady-state solutions $N_j/N_i = \rho_j/\rho_i$, corresponding to thermal equilibrium. If, in addition, rf fields are applied, we refer to the resulting steady-state condition as dynamic equilibrium. Take $W_{kl} \neq 0$ and all other $W_{ij} = 0$. The resulting rate equations may be solved directly, or they may be put into the following form:

$$I_i = 0 = \sum_{j \neq i} [(V_j - V_i)/R_{ij}],$$

$$i = 1, 2, \dots, n, \neq k, l, \quad (39a)$$

$$I_l = -I_k = \sum_{j \neq l} [(V_j - V_l)R_{jl}]$$

$$= - \sum_{j \neq k} [(V_j - V_k)/R_{jk}], \quad (39b)$$

if we define $R_{jk} = [w_{jk}\rho_j\rho_k]^{-1}$, $V_i = N_i/\rho_i$, and $I_l = (N_l - N_k)W_{kl}$. This result, previously obtained by Bloch²⁴ by a different method, shows that the rate equations are formally equivalent to the Kirchhoff equations Eqs. (39a) and (39b) for the net current I_i, I_k, I_l, \dots , out of each junction point i, k, l, \dots , of a network of resistors R_{ik}, R_{il}, \dots , where the potentials at the junction points are V_i, V_k, V_l, \dots . Thus the problem of finding the dynamic equilibrium populations is equivalent to finding the potentials in the passive network problem, subject to the normalization condition $\sum_i V_i \rho_i = \sum_i N_i = N$. We have used this method to calculate the resulting steady-state nuclear orientation in the following cases:

1. For the system of Fig. 3 the nuclear polarization is given to a good approximation by $p_1 = [N(\frac{1}{2}, \frac{1}{2}) + N(-\frac{1}{2}, \frac{1}{2}) - N(\frac{1}{2}, -\frac{1}{2}) - N(-\frac{1}{2}, -\frac{1}{2})]/\sum N_i$. Let us induce the forbidden transition $W_2(\frac{1}{2}, -\frac{1}{2} \rightarrow -\frac{1}{2}, \frac{1}{2})$ with a sufficient rf field to equalize the populations: $N(\frac{1}{2}, -\frac{1}{2}) = N(-\frac{1}{2}, \frac{1}{2})$; i.e., we saturate this transition.

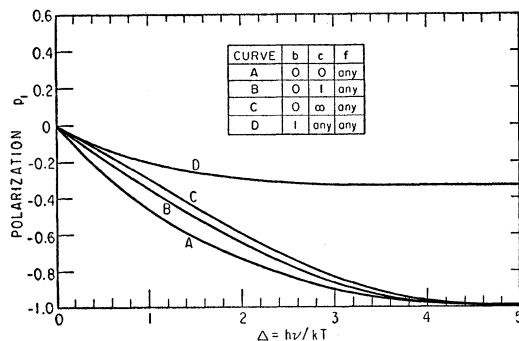


FIG. 4. Dynamic nuclear polarization p_1 versus Δ for saturation of the forbidden transition $W_2(\frac{1}{2}, -\frac{1}{2} \rightarrow -\frac{1}{2}, \frac{1}{2})$ of Fig. 3, for various relative values of relaxation transition probabilities.

²⁴ F. Bloch, Phys. Rev. **102**, 104 (1956).

Neglecting the hfs splitting $A/2$ in comparison to $g\beta H$ in the expressions for the Boltzmann factors, the resulting nuclear polarization in the first order approximation, $e^A \approx 1 + \Delta$, is

$$p_1 \approx \frac{(-\Delta/2)(1+c)}{2c+1+b}, \quad (40)$$

where $\Delta = h\nu/kT$. The exact behavior of p_1 with Δ is shown in Fig. 4 for various values of c and b . We note that p_1 is independent of f and not very sensitive to c ; p_1 is appreciably affected by b only if b approaches unity.

2. For the same system, Fig. 3, we instead induce strongly the allowed transition $W_1(\frac{1}{2}, \frac{1}{2} \rightarrow -\frac{1}{2}, \frac{1}{2})$ so that $N(\frac{1}{2}, \frac{1}{2}) = N(-\frac{1}{2}, \frac{1}{2})$. The resulting nuclear polarization to first order is

$$p_1 \approx \frac{(-\Delta/4)(f-c)(1+b)}{(1+b+c)(1+b+f)-1}. \quad (41)$$

We note that: for $c=b=0$, this polarization is half as large as that of Eq. (40); if $f \approx c$, p_1 vanishes; p_1 is appreciably reduced if b approaches f in value. The more exact behavior of p_1 with Δ is shown in Fig. 5 for selected values of c, f , and b ; it shows that at sufficiently large value of Δ there is a nonvanishing second order term in p_1 , even if $f=c$, etc.

3. For the hfs coupled system $I=1, S=\frac{1}{2}$ of Fig. 6, we calculate the nuclear alignment, given to a good approximation by

$$p_2 = [N(\frac{1}{2}, 1) + N(-\frac{1}{2}, 1) + N(\frac{1}{2}, -1) + N(-\frac{1}{2}, -1) - 2N(\frac{1}{2}, 0) - 2N(-\frac{1}{2}, 0)]/\sum N_i.$$

First we assume $b=0, c=0$ and saturate the allowed transition $W_1(\frac{1}{2}, 1 \rightarrow -\frac{1}{2}, 1)$. The resulting dynamic nuclear alignment is shown in Fig. 7(A). If, instead, we saturate the forbidden transition $W_2(-\frac{1}{2}, 1 \rightarrow \frac{1}{2}, 0)$ the resulting alignment is as in Fig. 7(B); etc. for the

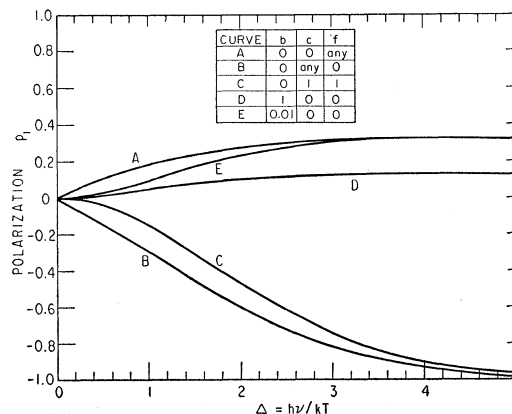


FIG. 5. Dynamic nuclear polarization p_1 versus Δ for saturation of the allowed transition $W_1(\frac{1}{2}, \frac{1}{2} \rightarrow -\frac{1}{2}, \frac{1}{2})$ of Fig. 3, for various relative values of relaxation transition probabilities.

other transitions. If the dc magnetic field H is slowly varied with constant applied rf frequency ν , the transitions corresponding to Fig. 7(A), 7(B), \dots , may be successively saturated and the resulting pattern of the steady-state nuclear alignment p_2 versus H is shown in Fig. 8 for the case $b=0$, $c=0$, which yields the maximum alignment. One finds that the alignment produced by the forbidden transitions is not appreciably reduced unless c and b become comparable to unity, whereas the alignment produced by the allowed transitions is, in first order, reduced to zero if $c \approx f$, or if $b \gg f$. The results are similar to those for p_1 in Figs. 4 and 5, and one draws these general conclusions:

Polarization or alignment produced by the saturation of the forbidden transitions is a process in which the nuclei are directly flipped (simultaneously with an electron) by the applied rf fields; since the transition probability for this process can, in principle, be made as large as desired by increasing the rf power, the competing relaxation processes, bw and cw in Fig. 3, do not appreciably reduce the orientation unless they are comparable to the major process w . On the other hand, the saturation of the allowed transitions produces in first order in Δ , an orientation only through a cross relaxation process, say fw . That is, the nuclei are indirectly flipped by a relaxation transition and the orientation is appreciably reduced if the competing relaxation processes cw and bw become comparable to fw ; this is a more severe restriction. For $\Delta \gtrsim 1$, second order effects partially nullify this advantage of using forbidden rather than allowed transitions. For example, Fig. 5(E) shows that at $\Delta \gtrsim 1$, saturation of the allowed transition will produce a polarization $p_1 \approx \frac{1}{3}$ even in complete absence of the cross relaxation transitions cw or fw .

In all of these methods the dynamic orientation is obviously reduced to zero at all values of Δ if $b \gg 1$;

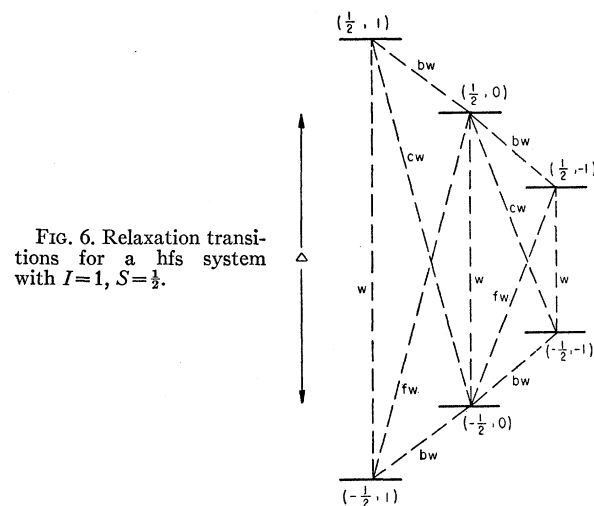


FIG. 6. Relaxation transitions for a hfs system with $I=1$, $S=\frac{1}{2}$.

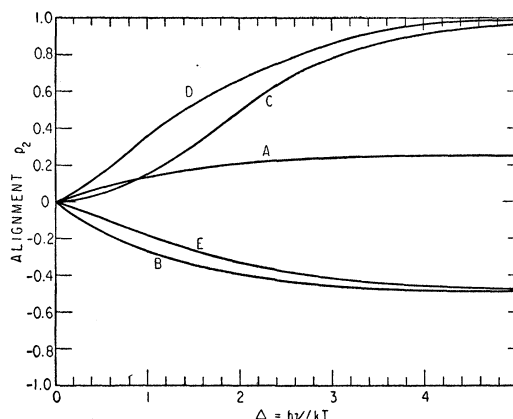


FIG. 7. Dynamic nuclear alignment p_2 versus Δ for rf saturation in Fig. 6 of these transitions: curve A, $W_1(\frac{1}{2}, 1 \rightarrow -\frac{1}{2}, 1)$; curve B, $W_2(\frac{1}{2}, 0 \rightarrow -\frac{1}{2}, 1)$; curve C, $W_1(\frac{1}{2}, 0 \rightarrow -\frac{1}{2}, 0)$; curve D, $W_2(\frac{1}{2}, -1 \rightarrow -\frac{1}{2}, 0)$; curve E, $W_1(\frac{1}{2}, -1 \rightarrow -\frac{1}{2}, -1)$. It is assumed $b=c=0$.

however, this is not a very realistic assumption, at least for paramagnetic ions in hydrated crystals.

For a general spin I in a system similar to Fig. 6 with $c=0$, $b=0$, the saturation of the forbidden transition $W_2(\frac{1}{2}, m \rightarrow -\frac{1}{2}, m+1)$ yields the polarization and alignment

$$p_1 = \frac{1}{2I} \frac{(e^{-\Delta} - e^{\Delta})[I(I+1) - m(m+1)]}{(1+e^{-\Delta})(I-m) + (1+e^{\Delta})(I+m+1)}, \quad (42)$$

$$p_2 = p_1(2m+1)/(2I-1).$$

The saturation of the allowed transition $W_1(\frac{1}{2}, m \rightarrow -\frac{1}{2},$

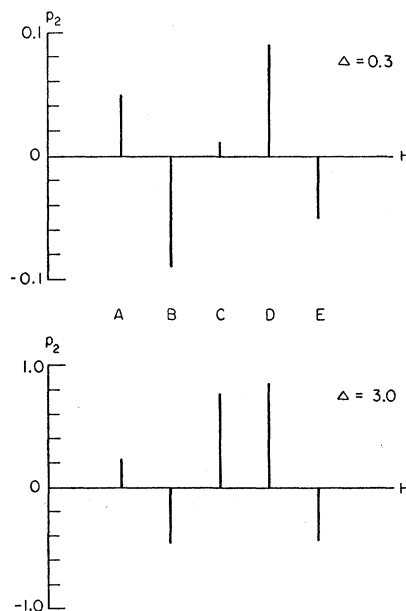


FIG. 8. Dynamic nuclear alignment p_2 versus field H for rf saturation, at two different values of Δ , of the transitions A, B, \dots , of Fig. 7.

m) yields

$$p_1 = \frac{1}{2I} \frac{(e^\Delta - e^{-\Delta})[I(I+1) - m(m+1)] + (1+e^{-\Delta})2m}{(1+e^{-\Delta})(I+m) + 2 + (1+e^\Delta)(I-m)}, \quad (44)$$

$$p_2 = \frac{1}{I(2I-1)} \frac{(e^\Delta - e^{-\Delta})(m+\frac{1}{2})[I(I+1) - m(m+1)] + (1-e^{-\Delta})[3m^2 - I(I+1)]}{(1+e^{-\Delta})(I+m) + 2 + (1+e^\Delta)(I-m)}. \quad (45)$$

We have considered only steady-state values of dynamic nuclear orientation. Pipkin and Culvahouse²⁵ have discussed the transient case, important in systems with long relaxation time, such as in doped silicon. We note further that dynamic orientation by forbidden transitions is in a rough sense the steady-state analog of Feher's²⁶ transient method using two successive adiabatic fast passage inversions of populations.

III. DIPOLAR COUPLING

The case of an electron and a nucleus in weak dipolar coupling in crystals has been discussed by Abragam,⁴ who showed that essentially no dynamic nuclear orientation was to be expected upon saturation of the usual allowed electron transitions. However, forbidden transitions which simultaneously flip an electron spin and a nuclear spin will indeed produce a dynamic polarization, as was first demonstrated by Abragam and Proctor¹¹ in a slightly modified way in a crystal of LiF: the nuclear spin involved was that of Li⁶ and the "electron spin" was in effect that of F¹⁹. The method has been used to obtain appreciable nuclear polarization of H¹,^{27,28} Si²⁹, F¹⁹,³⁰ and others. Here we are concerned principally with nuclear alignment, however.

We do not treat the general case of an electron spin surrounded by many nuclear spins, but instead take a simpler model in order to estimate the dynamic γ -ray anisotropy obtainable. Consider a single diamagnetic crystal containing a small fraction of paramagnetic ions and an even smaller fraction of some radionuclei of diamagnetic atoms, all at helium temperatures and in an external dc field H of a few thousand gauss. For a "typical pair" consisting of a paramagnetic ion \mathbf{S} and a radionucleus \mathbf{I} , separated by a distance \mathbf{r} , we take as the spin Hamiltonian in the principal coordinates ($x'y'z'$) of the ion g tensor

$$\mathcal{H} = g_{11}\beta S_{z'}(H_{z'} + D_{z'}) + g_{12}\beta[S_{x'}(H_{x'} + D_{x'}) + S_{y'}(H_{y'} + D_{y'})] + g_n\beta(H_{x'}I_{x'} + H_{y'}I_{y'} + H_{z'}I_{z'}) + \mathcal{H}_p, \quad (46)$$

²⁵ F. M. Pipkin and J. W. Culvahouse, Phys. Rev. **109**, 1423 (1958); J. W. Culvahouse and F. M. Pipkin, Phys. Rev. **109**, 319 (1958); F. M. Pipkin, Phys. Rev. **112**, 935 (1958).

²⁶ G. Feher, Phys. Rev. **103**, 500 (1956).

²⁷ E. Erb, J. L. Montchane, and J. Uebbersfeld, Compt. rend. **248**, 3050 (1958).

²⁸ J. Borghini and A. Abragam, Compt. rend. **248**, 1803 (1959); O. S. Leifson, P. L. Scott, and C. D. Jeffries, Bull. Am. Phys. Soc. Ser. II, **4**, 453 (1959).

²⁹ A. Abragam, J. Combrisson, and I. Solomon, Compt. rend. **247**, 2337 (1958).

³⁰ M. Abraham, M. A. H. McCausland, and F. N. H. Robinson, Phys. Rev. Letters **2**, 449 (1959).

where the magnetic dipolar field at \mathbf{S} due to \mathbf{I} is given by $\mathbf{D} = g_n\beta r^{-3}[\mathbf{I} - 3\mathbf{r}\mathbf{r}^{-2}(\mathbf{I}\cdot\mathbf{r})]$, and \mathcal{H}_p is the nuclear electric quadrupole interaction of \mathbf{I} . For simplicity we omit all other interactions of the paramagnetic ion.

We transform Eq. (46) to the laboratory coordinates (x,y,z ; r,θ,φ) as in Sec. II A for $z'\parallel z\parallel H$. For \mathcal{H}_p , $g_{11}\beta D \ll g_n\beta H$, the first order wave functions are

$$\psi_{11}(M,m) = d_0\psi^0(M,m) + d_+\psi^0(M,m+1) + d_-\psi^0(M,m-1), \quad (47a)$$

where

$$d_{\pm} = \pm(\frac{3}{2})g_{11}\beta r^{-3}H^{-1}\sin\theta\cos\theta M r_{\mp}\exp(\mp\varphi). \quad (47b)$$

An applied rf field, Eq. (16), induces the allowed transitions W_1 given by Eq. (21), and in addition, the forbidden transitions

$$W_2(M, m \rightarrow M \pm 1, m \mp 1) = W_1 r_{\pm}^2 \sigma^2 \text{ sec}^{-1}, \quad (47c)$$

$$W_3(M, m \rightarrow M \pm 1, m \pm 1) = W_1 r_{\mp}^2 \sigma^2 \text{ sec}^{-1}, \quad (47d)$$

where $\sigma = (\frac{3}{2})g_{11}\beta r^{-3}H^{-1}\sin\theta\cos\theta$.

For $z'\perp H$ one obtains ψ_1 by replacing g_{11} by g_1 in ψ_{11} ; and rf perturbation, Eq. (17), induces the allowed transitions W_1 of Eq. (24) and the forbidden transitions obtained from Eqs. (47c) and (47d) by replacing g_{11} by g_1 in the expression for σ . Thus anisotropic ions where $g_1 \gg g_{11} \approx 0$ may be used for inducing the transitions W_2 and W_3 if one takes the orientation $z\parallel H \perp z'\perp H_1$.

The energy levels are shown in Fig. 9 for the case $S=\frac{1}{2}$, $I=1$. The transitions W_2 and W_3 were first observed by Livingston and Zeldes³¹ and appear on the paramagnetic resonance spectra as two satellite lines spaced $\pm g_n H/g$ gauss about the main transition line W_1 . The relative intensity is of order $W_2/W_1 \sim \sigma^2 \sim 10^3 r^{-6} H^{-2}$, where r is in angstroms and H in gauss. For $r \sim 10$ Å, characteristic for a paramagnetic ion concentration of $\sim 10^{-2}$, and $H \sim 10^4$ gauss, the relative intensity $\sigma^2 \sim 10^{-6}$ is too small to permit direct observation of W_2 and W_3 but they may nevertheless be effective in dynamic nuclear orientation if they are theoretically resolved, which, for the moment we assume: the electronic line width $\Delta H \ll g_n H/g$.

We assume^{4,32} that the important relaxation processes are represented by the first, second, third, and fifth terms of Eq. (34); i.e., we neglect the fluctuations in the dipolar coupling. The principal relaxation transitions will be: $w_1(M, m \rightarrow M \pm 1, m)$ and $w_2(M, m \rightarrow M \pm 1,$

³¹ H. Zeldes and R. Livingston, Phys. Rev. **96**, 1702 (1954); G. J. Trammell, H. Zeldes, and R. Livingston, Phys. Rev. **110**, 630 (1958).

³² N. Bloembergen, Physica **15**, 386 (1949).

$m \mp 1) = w_3(M, m \rightarrow M \pm 1, m \pm 1)$ due to the first and second terms (electronic); and $w_4(M, m \rightarrow M, m \pm 1)$ and $w_7(M, m \rightarrow M, m \pm 2)$ due to the third and fifth terms (nuclear). These relaxation transitions are represented schematically in Fig. 9, where f , b , and d are dimensionless parameters; we expect $f \sim \sigma^2$, and b and d to be determined by residual paramagnetic impurities and quadrupole interactions.

Let us saturate the three coincident allowed transitions $W_1(\frac{1}{2}, 1 \rightarrow -\frac{1}{2}, 1)$, $W_1(\frac{1}{2}, 0 \rightarrow -\frac{1}{2}, 0)$, and $W_1(\frac{1}{2}, -1 \rightarrow -\frac{1}{2}, -1)$ in Fig. 9. Then the populations of all the levels become equal in the steady state and the dynamic nuclear orientation remains zero for all values of $\Delta = \hbar\nu/kT$.

Let us, instead, saturate the two coincident forbidden transitions $W_2(\frac{1}{2}, 0 \rightarrow -\frac{1}{2}, 1)$ and $W_2(\frac{1}{2}, -1 \rightarrow -\frac{1}{2}, 0)$. If $b, d, f \ll 1$ the steady-state dynamic populations take the values shown in Fig. 9(a), corresponding to a nuclear polarization $(p_1)_{w_2} = (1 + e^{-\Delta} - e^{\Delta} - e^{2\Delta}) / (2 + 2e^{\Delta} + e^{-\Delta} + e^{2\Delta}) \approx -(\frac{2}{3})\Delta$ and to a nuclear alignment

$$(p_2)_{w_2} = (e^{-\Delta} - e^{\Delta} - 1 + e^{2\Delta}) / (2 + 2e^{\Delta} + e^{-\Delta} + e^{2\Delta}) \approx \Delta^2/3.$$

If instead of W_2 we saturate the two forbidden transitions $W_3(\frac{1}{2}, 1 \rightarrow -\frac{1}{2}, 0)$ and $W_3(\frac{1}{2}, 0 \rightarrow -\frac{1}{2}, -1)$, the populations become those of Fig. 9(b), corresponding to a polarization $(p_1)_{w_3} \equiv -(p_1)_{w_2}$ and an alignment $(p_2)_{w_3} \equiv (p_2)_{w_2}$. Thus the polarization is reversed, but the alignment, being only a Δ^2 effect, is not. At a frequency $\nu \sim 3 \times 10^{10}$ cps and a temperature $T \sim 1^\circ\text{K}$, the second order alignment is considerable, however, and would yield γ -ray anisotropies of $\sim 10\%$, typically.

It is clear that the values of p_1 and p_2 thus calculated are optimum values and will be appreciably reduced if b or d or f become comparable to unity.

In the event that the electronic line is homogeneously broadened over a width $\Delta H \gg g_n H/g$, the transitions W_1 , W_2 , and W_3 can essentially occur simultaneously throughout the sample, equalizing the populations, with a negligible resultant nuclear orientation. However, if the line is inhomogeneously broadened³³ a polarization is observed,^{29,30} reduced by a differential effect due to the fact that $(p_1)_{w_3} \equiv -(p_1)_{w_2}$. Since $(p_2)_{w_2} \equiv (p_2)_{w_3}$ one would not expect a corresponding differential reduction in the alignment and the γ -ray anisotropy. For an inhomogeneously broadened line width $\Delta H \gtrsim g_n H/g$ it may be possible at feasible rf powers to sweep through the line, saturating the W_2 and W_3 transitions, in a time short compared to the times $\sim (fw)^{-1}$, $(bw)^{-1}$, $(dw)^{-1}$ required for the saturation of the W_1 transition to destroy the alignment produced by W_2 and W_3 .

Finally, if we consider the case where the quadrupole term \mathcal{H}_q in Eq. (46) is comparable to the nuclear Zeeman term, then the $(\frac{1}{2}, m)$ levels and the $(-\frac{1}{2}, m)$ levels in Fig. 9 are no longer equally spaced. Instead of two, there are four forbidden satellites about the main

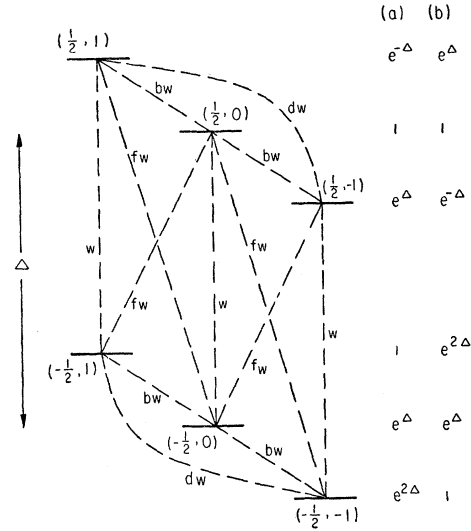


FIG. 9. Magnetic energy levels (M, m) and relaxation transitions for $S = \frac{1}{2}$ and $I = 1$ in weak dipolar coupling. Column (a) gives the populations for rf saturation of forbidden transitions W_2 , Eq. (47c), assuming $b, d, f \ll 1$. Column (b) is for saturation of transitions W_3 , Eq. (47d).

line. Saturation of any one of them produces a first order term Δ in the alignment.

IV. γ -RAY ANISOTROPY

The angular distribution of γ radiation from oriented nuclei has been adequately treated¹⁰ and we use the results and notation of Steenberg.³⁴ Consider a system of nuclear spins distributed over a set of magnetic energy levels of the types in II or III above, where N_i is the population of the i th level. Assume, for the moment, that m_i is a good quantum number: $\langle \psi_i | I_z | \psi_i \rangle = m_i$. If the nuclei are radioactive and decay by emission of a series of γ -rays and particles, the angular distribution of a given γ -ray transition can be written in the form:

$$G(\theta) = \sum_i N_i G m_i(\theta) / \sum_i N_i, \quad (48a)$$

$$G_m(\theta) = 1 + \sum_k \alpha_k \Pi_k(m, I) P_k(\theta), \quad k = 2, 4, \dots, 2p. \quad (48b)$$

Here θ is the angle between the γ -ray detector and the z axis; the α_k are nuclear parameters given explicitly by Steenberg,³⁴ which depend on the various angular moments involved in the decay scheme; the $P_k(\theta)$ are the Legendre polynomials: $P_1 = (\frac{3}{2}) \cos^2 \theta - (\frac{1}{2})$, $P_2 = (\frac{3}{8}) \times [(35/3) \cos^4 \theta - 10 \cos^2 \theta + 1]$, etc. The Π_k are essentially Clebsch-Gordan coefficients and have the property

$$\sum_{m=-I}^I \Pi_k = 0,$$

the first two being $\Pi_2(m, I) = 3m^2 - I(I+1)$, and $\Pi_4(m, I) = (\frac{1}{12}) [35m^4 - 5(6I^2 + 6I - 5)m^2 + 3I(I+1)(I+2)(I-1)]$.

³³ A. M. Portis, Phys. Rev. **91**, 1071 (1953).

³⁴ N. R. Steenberg, Proc. Phys. Soc. (London). **A65**, 791 (1952).

The upper value of k is restricted to $2p$, where p is the smallest of the various angular momenta involved in the decay scheme, including those of the initial and intermediate nuclear states and the γ -photon. We restrict our discussion to $k=2, 4$, which is sufficient to include dipolar and quadrupolar radiations.

For the system of II the angular distribution $G(\theta)$ will show an anisotropy even in the absence of a dynamic nuclear orientation because of the various static orientation processes. In the usual static orientation experiment one observes the temperature variation of this anisotropy at very low temperatures, in order to determine, say the hfs coupling constants and the nuclear spin. It is convenient to do dynamic orientation experiments at a constant temperature in the liquid helium range, where the anisotropy from static processes is usually quite small and negligible in comparison to that from dynamic processes. Then it is useful to define a dynamic anisotropy

$$\epsilon = [G(\pi/2) - G(0)]/G_0, \quad (49)$$

where $G(\pi/2)$ and $G(0)$ are the γ -ray counting rates in the directions perpendicular and parallel to the H field (z axis), respectively, under conditions of dynamic orientation, and G_0 is the average (essentially isotropic) counting rate in the absence of dynamic orientation. This differs somewhat from the usual definition of anisotropy, but it is the parameter actually measured in our experiments.^{8,9} The anisotropy can be re-written

$$\epsilon = (-\frac{3}{2})\alpha_2 p_2' - (\frac{5}{8})\alpha_4 p_4', \quad (50)$$

where

$$p_k' = \sum_i N_i \Pi_k(m_i) / \sum_i N_i, \quad k=2, 4. \quad (51)$$

It is seen that the alignment p_2 defined in Eq. (2) is simply a normalized generalization of p_2' to include the case where m_i is not a good quantum number; etc. for p_4, p_4' . If p_4 or α_4 are negligible, and the forbidden

transition $W_2(\frac{1}{2}, -I \rightarrow -\frac{1}{2}, -I+1)$ is saturated, $\epsilon \approx -3\Delta\alpha_2 I(2I-1)(2I+1)^{-1}$, which has the typical order of magnitude $\epsilon \sim 0.05$ for $\Delta = h\nu/kT \sim 0.3$, $\alpha_2 \sim 0.05$, $I \sim 2$. If the various transitions, forbidden and allowed, are in turn saturated by varying the dc field at constant frequency a γ -ray anisotropy pattern similar to the p_2 pattern of Fig. 8 will be observed, from which the spin I and the hfs constant A may be directly determined. In effect the paramagnetic resonance spectrum is observed through the γ -rays, an idea suggested by Bloembergen and Temmer.³⁵

To estimate the sensitivity of this type of experiment we note that the number of nuclear decays necessary is of order $D \sim (s/\epsilon)^2 (C/F)$, where s is the signal to noise ratio in observing an anisotropy ϵ in each of a total of C "channels" of the resonance spectrum, and F is the γ -ray loss factor due to geometry and detector inefficiency. With the typical values $s \sim 10$, $\epsilon \sim 0.01$, $F \sim 0.003$, $C \sim 100$, the total number of decays required is of order $D \sim 3 \times 10^{10}$. For a half-life of a few hours we may equate this number to the minimum number of radionuclei required; this is to be compared to direct paramagnetic resonance absorption where approximately 10^{14} nuclei are required in a typical experiment.

V. COMPARISON WITH EXPERIMENTS

In Table I are briefly summarized some of the results at Berkeley of Abraham et al.,^{6,8} and Kedzie et al.,^{7,9} in attempts to dynamically orient radionuclei of paramagnetic ions in strong hyperfine coupling, Sec. II. Several crystal structures with widely differing paramagnetic parameters are represented. All the experiments were performed at an rf frequency of $\nu \approx 9 \times 10^9$ cps and a temperature $T \approx 1.5^\circ\text{K}$. For each case, all the γ -rays in the total decay scheme were counted in measuring the anisotropy. The counting rate was such that an anisotropy $\epsilon \geq 10^{-3}$ would have been detected.

TABLE I. Summary of dynamic nuclear orientation experiments on radionuclei at Berkeley (Abraham et al.,^a and Kedzie et al.,^b).

Experiment No.	Nucleus	Crystal	Paramagnetic parameters	γ -ray ϵ observed
1	Co ⁶⁰	La ₂ Mg ₃ (NO ₃) ₁₂ · 24 D ₂ O, site I	$g_{11} \approx g_1 \approx 4.3$; $A \approx B \approx 0.006 \text{ cm}^{-1}$	$\sim 1\%$
2	Co ⁶⁰	La ₂ Mg ₃ (NO ₃) ₁₂ · 24 D ₂ O, site II	$g_1 \sim 8$, $g_{11} \sim 2$; $A \approx 0.018 \text{ cm}^{-1}$, $B \approx 0$	0
3	Mn ^{52,54}	La ₂ Mg ₃ (NO ₃) ₁₂ · 24 H ₂ O, site I	$D \approx 0.025 \text{ cm}^{-1}$; $A(54) \approx B(54) \approx 0.0075 \text{ cm}^{-1}$ $g_1 \approx g_{11} \approx 2$; $A(52) \approx B(52) \approx 0.0035 \text{ cm}^{-1}$	~ 0
4	Mn ^{52,54}	La ₂ Mg ₃ (NO ₃) ₁₂ · 24 H ₂ O, site II	$D \approx 0.006 \text{ cm}^{-1}$; $A(54) \approx B(54) \approx 0.0075 \text{ cm}^{-1}$ $g_1 \approx g_{11} \approx 2$; $A(52) \approx B(52) \approx 0.0035 \text{ cm}^{-1}$	$\sim 1\%$
5	Ce ¹⁴¹	La ₂ Mg ₃ (NO ₃) ₁₂ · 24 H ₂ O	$g_{11} \sim 0.2$, $g_1 \approx 1.8$; $A \sim 0$, $B \approx 0.013 \text{ cm}^{-1}$	0
6	Np ^{238,239}	UO ₂ Rb(NO ₃) ₃	estimated: $A \sim 0.1 \text{ cm}^{-1}$ $B \sim 0.01 \text{ cm}^{-1}$ $g_{11} \approx 3.4$, $g_1 \approx 0$ $P \sim 0.03 \text{ cm}^{-1}$	0

^a See footnotes 6 and 8.

^b See footnotes 7 and 9.

³⁵ N. Bloembergen and G. Temmer, Phys. Rev. **89**, 883 (1953).

If Co^{2+} ions are substituted for Mg in $\text{La}_2\text{Mg}_3(\text{NO}_3)_{12} \cdot 24\text{H}_2\text{O}$, there are two possible sites, magnetically unequivalent. In experiment 1, Table I, we are concerned with Co^{60} in the almost isotropic site. A γ -ray anisotropy of $\epsilon \sim 0.01$ was observed when the forbidden transitions W_2 , Fig. 2, were saturated. Essentially no ϵ was observed for saturation of the allowed transition W_1 ; this is probably because of appreciable relaxation transitions cw or bw , Fig. 6, as discussed in Sec. II B above.

In experiment 2, we consider Co ions in the other, very anisotropic, site in the same crystal. No γ -ray ϵ for saturation of either forbidden or allowed transitions was observed. We explain this as follows: For $z \parallel H$, approximately, the transition probability W_2 is too small because of the size of B to allow for the forbidden transitions to be saturated. For $z \perp H$, approximately, we see from Eqs. (25) and (26) that since $A \gg B$, $W_2 \approx W_3$. These would give rise to equal but opposite alignments at very nearly the same dc field resulting in a greatly reduced net anisotropy. Dynamic nuclear alignment by saturation of allowed transitions fails probably for similar reasons: $f \ll b$ at $z \parallel H$ and $c \approx f$ at $z \perp H$.

If Mn^{2+} is substituted for Mg^{2+} in the double nitrate, two sites are possible, one with a considerably larger zero-field splitting than the other. In experiment 3 no clearly detectable ϵ was observed for radioactive Mn^{52} or Mn^{54} at the site with the larger splitting. In experiment 4, for the site with small splitting, anisotropies of the order $\epsilon \sim 10^{-2}$ were observed corresponding to saturation of either types of forbidden transitions W_2 or W_3 , which occur in the case of Mn^{54} at appreciably different dc fields; also saturation of the allowed transition W_1 produced an anisotropy. These experi-

ments have resulted in a measurement of the nuclear moments: $I(\text{Mn}^{52})=6$, $|\mu(\text{Mn}^{52})|=3.00 \pm 0.15$ nm, $I(\text{Mn}^{54})=3$, $|\mu(\text{Mn}^{54})|=3.29 \pm 0.06$ nm.

In experiment 5, Ce^{141} was substituted for La in the double nitrate crystal. Since $g_{11} \sim 0.2$ required a dc field higher than was available the forbidden and allowed lines were saturated in the orientation $z \perp H$. No γ -ray ϵ was observed, probably because the inequality $B \gg A$ makes $W_2 \approx W_3$; these transitions would be nearly superposed for Ce^{141} .

In experiment 6, Np^{238} and, separately, Np^{239} were substituted for U in a uranyl rubidium nitrate crystal. No γ -ray ϵ was observed for the approximate orientation $z \parallel H$ by saturation of either the allowed or forbidden transitions. Possibly the appreciable quadrupole interaction P in this case makes the relaxation process bw stronger than any others, significantly reducing the maximum alignment attainable.

Many miscellaneous pieces of information point to spectral diffusion³⁶⁻³⁸ effects as additional and independent reasons for the failure to observe an alignment in some cases.

ACKNOWLEDGMENTS

It is a great pleasure to thank: The National Science Foundation for a Senior Post-Doctoral Fellowship and The Clarendon Laboratory, Oxford, for hospitalities; B. Bleaney for many helpful suggestions; the U. S. State Department for a Fulbright Research Scholarship and the Centre d'Etudes Nucléaires de Saclay for courtesies extended; and A. Abragam for numerous informative discussions.

³⁶ A. M. Portis, Phys. Rev. **104**, 584 (1956).

³⁷ N. Bloembergen, S. Shapiro, P. S. Pershan, and J. O. Artman, Phys. Rev. **114**, 445 (1959).

³⁸ P. G. deGennes, J. Phys. Chem. Solids **7**, 345 (1958).